DOI: https://doi.org/10.1007/s40415-023-00937-1

Brazilian Journal of Botany (2023) 46:799–813
https://doi.org/10.1007/s40415-023-00937-1

BIOCHEMISTRY & PHYSIOLOGY - ORIGINAL ARTICLE

Leaf anatomy and dereplication by FIA-ESI-IT-MS/MS of secondary metabolites of *Clusia criuva* Cambess as an integrative approach to assess the environmental status of coastal plain forests

Leonardo M. de Souza Mesquita[1,2] · **Vinícius Filipe Fernandes Pereira**[1] · **Beatriz Zachello Nunes**[3,4] · **Marilia Nagata Ragagnin**[5] · **Marcelo M. Pereira Tangerina**[6] · **Cláudia Quintino da Rocha**[7] · **Odair José Garcia de Almeida**[1] · **Maria Bernadete Gonçalves Martins**[1] · **Wagner Vilegas**[1]

Received: 7 March 2023 / Revised: 7 September 2023 / Accepted: 8 September 2023 / Published online: 21 September 2023

Abstract

The increasing development of industry, ports, tourism, and commerce along the coasts poses a severe threat to local forests due to elevated levels of pollutants. An effective way to assess the impact of this contamination is by evaluating living organisms' anatomical features and chemical composition. This research examined the potential of *Clusia criuva* Cambess leaves as a bioindicator model for screening sandy coastal plain forests (Restingas). The study collected samples from pristine (PA) and disturbed (DA) areas, confirmed through literature review and sediment concentration by guidelines analysis. Microscopy images of the leaves revealed that PA samples are thicker and have fewer druse crystals than DA. Mass spectrometry fingerprint analysis identified key compounds such as flavonoids, benzophenones, and phenolic acids (FIA-ESI-IT-MS/MS), which could be considered chemical markers from the genus. The chemical composition of extracts from PA and DA differed significantly, with a low similarity index (40%). Quinic acid derivatives are found only in plants from PA, which may be a response against intense herbivory agents. Instead, 7-*epi*-nemerosone, was detected only samples from DA, probably due to the need to defend against oxidative stressors. Besides, the similarity between each study area's three distinct sampling points was around 80%, indicating low chemical variability within the exact location. This study demonstrates an integrative methodology for assessing and supporting the environmental status of Restinga ecosystems, ensuring a comprehensive response that can promote conservation strategies.

Keywords *Clusia criuva* Cambess · Coastal plain forests · Environmental monitoring · Leaf anatomy · Secondary metabolites

1 Introduction

The sandy coastal plain forests (known as *Restinga*) are a distinct physiognomy located near the seacoast in the Brazilian Atlantic Rainforest, characterized by plants ranging from sparse to transitional broadleaves (Rocha et al. 2007). However, the preservation of this ecosystem is under threat due to anthropogenic disturbances resulting from real estate expansion, ports, businesses, and industries (Defeo et al. 2009; Harris et al. 2015). Additionally, the sandy coastal

✉ Leonardo M. de Souza Mesquita
mesquitalms@gmail.com

[1] Institute of Biosciences, São Paulo State University (Unesp), São Vicente, SP, Brazil

[2] Multidisciplinary Laboratory of Food and Health (LabMAS), School of Applied Sciences (FCA), University of Campinas, Rua Pedro Zaccaria 1300, Limeira, Sao Paulo 13484-350, Brazil

[3] Instituto Do Mar, Universidade Federal de São Paulo (IMAR -UNIFESP), Santos, SP, Brazil

[4] Instuto de Oceanografia, Universidade Federal Do Rio Grande (IO-FURG), Rio Grande, RS, Brazil

[5] Oceanographic Institute, University Of São Paulo, São Paulo, SP 05508-120, Brazil

[6] Departamento de Botânica, Instituto de Biociências, Universidade de São Paulo, São Paulo, SP 05508-090, Brazil

[7] Laboratório de Química de Produtos Naturais (LQPN), UFMA–Federal University Of Maranhão, Av. Dos Portugueses, 1966, Bacanga, São Luís, MA 65080-805, Brazil

plain and estuarine ecosystems face stressful conditions such as sandy and unconsolidated soil, high ultraviolet radiation, water shortages, and saline sprays, which can affect the production of secondary metabolites in their plants (de Souza Mesquita et al. 2018; Scarano 2009). Certain plant biomarkers are specific to pollutants or pollutant groups, while others respond to various pollutants and/or stressors. For example, the accumulation of flavonoids, phenolic acids and terpenoids can indicate plant stress and reflect the presence of pollutants or alterations in environmental conditions (Azzazy 2020).

The Clusiaceae family is one of the most significant plant families in the coastal ecosystem (Rocha-Filho et al. 2012). It comprises 800 species and 14 genera, divided into three tribes, namely Clusieae, Garcinieae, and Symphonieae, representing 93% of the family (Gustafsson et al. 2002, 2007). The genus *Clusia* plays a crucial role in ecological succession, acting as an intermediary plant that can establish itself even under extreme environmental conditions. The genus is also known for its unique physiological and anatomical adaptations that prevent water loss (xeromorphic characteristics), such as Crassulacean Acid Metabolism (CAM), oblong leaves with thick epicuticular wax, high stomata density, thick palisade parenchyma, presence of hypoderm, and high trichome density (Barrera Zambrano et al. 2014; Boeger and Wisniewski 2003; Lüttge 2010). Besides, *Clusia* leaves are abundant in diverse secondary metabolites, encompassing polyprenylated benzophenones, terpenoids, benzoquinones, and flavonoids. Vitexin derivatives, a widely occurring flavonoid in the *Clusia* genus, have been recognized as a valuable chemotaxonomic marker (Compagnone et al. 2008). Moreover, its efficacy in combating oxidative stress-related diseases has been established (Babaei et al. 2020). Besides the phenolic compounds, benzophenones (terpenoids) hold significant medicinal value (Masyita et al. 2022). Also, they could be a significant environmental indicator once associated with plant stress, such as herbivory, pathogen attack, or environmental pollution. These chemotaxonomic compounds contribute to the extensive chemical diversity observed within the *Clusia* genus, thereby serving as valuable markers for assessing the environmental status of coastal plain forests.

Coastal regions are known for their inherent environmental disturbances, making some plants act as bioindicators to screen the preservation status of the ecosystem (Rahman et al. 2023). These bioindicators exhibit quantifiable and predictable changes in their vital functions, chemical composition, morphology, and anatomy, which can help assess the environment's quality (Parmar et al. 2016). Numerous studies have already illustrated the bioindicator potential of leaf anatomical features in *Clusia* spp. For instance, *C. hilariana* has been established as a reliable bioindicator of atmospheric pollutants emitted by the pelletizing factory (da Silva et al. 2015, 2017b); and even as a bioindicator of acid rains, as exposed in an experimental study performed by (da Silva et al. 2005), putting the genus *Clusia* as an excellent choice to take an accurate snapshot of the environmental status as a bioindicator model. This becomes more realistic when integrative studies evolving anatomic and chemical profiles are done, filling the knowledge gaps about the phytochemistry and biology of this explored ecosystem.

It is imperative to undertake comparative investigations between polluted and unpolluted regions to safeguard and maintain these habitats and foster a comprehensive understanding of pollution and neglect issues. In this context, the central aim of this research was to carry out an integrative and comparative analysis using *C. criuva* Cambess leaves as a new bioindicator model, comparing a pristine habitat with a disturbed one within sandy coastal ecosystems. To achieve this goal, we scrutinized the leaf anatomical features and the predominantly secondary metabolites that act as indicators of the environment's quality, providing new instruments for environmental monitoring.

2 Material and methods

Plant material – To compare the foliar anatomy and secondary metabolites composition in *C. criuva*, we collected leaves from two different regions (one pristine and one disturbed area) on the central coast of São Paulo State, Brazil (Fig. 1a). The samples were collected in the same period (Spring season of the southern hemisphere) in both areas to avoid some seasonal interference with the results. In each location, the same collection approach was performed; we randomized three collection points (P1, P2, and P3), and then, in order to mitigate the effect of light exposure and herbivory, we collected leaves from the central branch at 100 cm from the substrate ($n > 200$) from 10 *C. criuva* specimens, vegetative stage, from each point (around 20 leaves from each plant). After collection, the samples were lyophilized to stop biochemical reactions and preserve the metabolite profile, then powdered in a ball mill and sieved through a #60 mesh. The voucher materials, including the three replicas of the two areas, were deposited at the Herbarium UNISANTA under the international access number HUSC—8.150.

Pristine area (PA) – The *Juréia-Itatins* Ecological Station (JIES) is a mosaic of Conservation Units, located on the south coast of Peruíbe city, São Paulo State, Brazil, and was used as a model of a pristine area (PA) (Fig. 1). This protected area is commonly used as a reference of a pristine area in studies evaluating the effects of anthropogenic stressors (e.g. Duarte et al. 2019; Petracco et al. 2015) since human activities and access are restricted. In general, the JIES

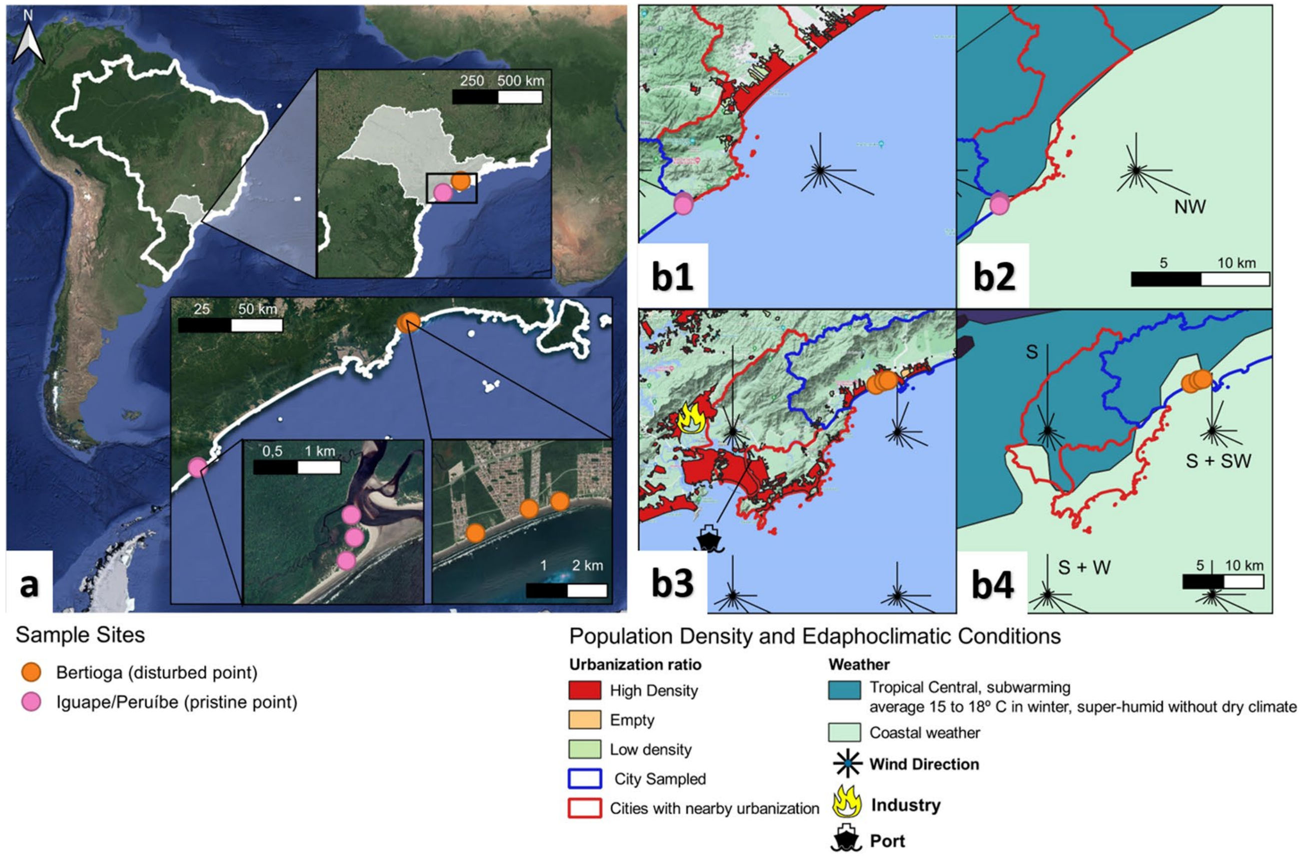

Fig. 1 **a** Sampling stations in pristine and disturbed points in Brazilian Southeast beaches, **b1** and **b3** the terrestrial landscape and urban density characterization, and **b2** and **b4** the weather and wind direction representation

region is characterized by small settlements of traditional communities, high conservation status, and lower levels of contamination and anthropogenic impacts of the São Paulo coast (Cruz et al. 2019). The study area is inserted in the south Una river bank (Fig. 1). In contrast to the disturbed area (characterized below), the sampled area in PA does not have the influence of air pollution from the nearby north urbanization (Peruíbe) due to the annual wind direction rate, which indicates a drag-away influence of the city (Fig. 1). The climate in PA is predominantly tropical and super humid, with the additional influence of coastal weather. Still, studies showed good to high ecological quality status in estuarine areas (Moreira et al. 2019) and low metal concentrations in mangrove areas (Pinheiro et al. 2013), as well as low concentrations of organic pollutants in sandy beaches (Taniguchi et al. 2016). Samples were collected from three distinct points (PA_{P1}, PA_{P2}, and PA_{P3} – pink dots) in the coastal plain forests of the Barra do Una area, located in the municipality of Peruíbe city, inside the JIES (Fig. 1).

Disturbed area (DA) – The sampling area from the coastal plain forest inside the São Lourenço beach (Bertioga, São Paulo State, Brazil) was used as a disturbed area (DA). This area is located north of the Bertioga Channel and, therefore, nearby the Port of Santos and the Industrial Complex of Cubatão city, potential sources of pollutants for the surrounding region. The port and the adjacent Cubatão city industrial complex contribute to the discharge of contaminants and marine litter into the region (Izar et al. 2019). Also, the region is surrounded by the Serra do Mar slope, which significantly affects pollution levels, resulting in worse air quality and wet deposition, and even though SO_2 concentrations in Cubatão remain a concern despite significant emission reductions since the 1980s, with local sources playing a significant role in wet deposition chemistry (Vieira-Filho et al. 2015) (Fig. 1). As well as in PA, the DA weather is tropical and super humid, influencing coastal weather. Using plants as bioindicators of air pollution at the Serra do Mar near the industrial complex of Cubatão was applied and proved to be a helpful indicator in the area (Klumpp et al. 1994). Also, the area is characterized by solid real-estate pressure and higher urbanization than the pristine area due to the Riviera de São Lourenço district (Fig. 1). The district was planned to be a residential and commercial project with high tourist appeal. Although São Lourenço locality has good sanitary and balneability conditions (CETESB), areas naturally occupied by sandy coastal species, such as *C. criuva* were suppressed by urban development (Fig. 1c), and an intense erosive process occurs along the beach. Thus, samples were collected in three distinct areas in the DA, namely DA_{P1}, DA_{P2}, and DA_{P3} (Fig. 1).

Climate characterization – Figure S1 (Supplementary Material) illustrates the monthly temperature and rainfall fluctuations over a continuous 31-day period around each day of the year. Both Iguape/Peruíbe (PA) and Bertioga (DA) undergo significant seasonal variations in monthly rainfall throughout the year, with January being the wettest month, receiving an average of 216 mm of rainfall. Conversely, August is the least rainy month, averaging 51 mm rainfall. In terms of temperature, both areas experience a range of 18 °C to 25 °C during winter and 25 °C to 31 °C during summer. Notably, the climate in both studied regions exhibits striking similarities, thereby providing a basis for comparing them in terms of anthropization and pollution, which are huge differences. All the data regarding climate characterization were acquired directly in the website of the *Instituto Nacional de Meterologia, Ministério da Agricultura e Pecuária–Brazil* (portal.inmet.gov.br/).

Review of peer-reviewed literature and environmental risk assessment – To assess the occurrence of contaminants in both PA and DA, a structured approach with seven different steps was performed: (1) study area delimitation, (2) bibliographic survey, (3) construction of attribute tables, (4) data insertion in a Geographic Information System (GIS), (5) identification of the presence of contamination residues and, (6) impacts appraisal using the outcomes against specific environmental quality guidelines/directives. Peer-reviewed articles were searched using the TOPIC = "Contamination + [name of the city]", that means "Juréia", "Bertioga", "Guarujá", "Cubatão", "São Vicente", "Santos", "Peruíbe", "Iguape" and "Cananéia" as keywords in the Science Direct, and Web of Science. Published papers were selected considering studies performed in the selected coastal areas (Fig. 1). Based on the scientific literature and providing georeferenced data on sediment and/or biota levels, a database was constructed, including concentrations of each substance on a site-by-site basis. The selected time frame considered only data from samples obtained between 2002 and 2017. Also, since there are no local guidelines for metal contamination and other substances in sediment, the Brazilian Criteria (CONAMA and CETESB) are based on the Canadian Environmental guidelines, which were grounded by Long et al. (1995). The estimative of impacts was based on intervals of effect-range low (ERL) and effect-range medium (ERM), commonly used to assess environmental quality through the concentration of contaminants in sediments. According to Long et al. (1995), the results were categorized since they represent a safe range expressed in concentration values that induce occasional effects in organisms. The georeferenced database was imported into QGis software. According to the guideline's evaluation, the number of records near each collection point allowed graphical visualization of the occurrence and identification of critical areas.

Anatomical analysis *Light microscopy*. All plant material was fixed in a solution of FAA 50 (1:1:18, formalin, acetic acid, ethanol 50% (v:v), respectively), and then transferred to an aqueous solution of ethanol 70% (v:v) (Johansen 1940). The resulting material was dehydrated in an ethanol series, embedded in Leica® Historesin (according to manufacturers' instructions), and then cross-sectioned at 7–8 µm thicknesses with a rotary microtome (Leica® RM 2255). Sections were stained with toluidine blue O, following (O'Brien et al. 1964). The slides were covered with coverslips and synthetic resin Entellan®. Images were taken under a light and polarized microscope equipped with a capture image system (Zeiss Primo Star®). Plates of images were edited, labelled, and assembled using Adobe Photoshop CS3, and Axion Vision–Zeiss software®. A total of 30 leaves of each point (pristine–PA_{P1}, PA_{P2}, and PA_{P3}; and disturbed–DA_{P1}, DA_{P2}, and DA_{P3}) were analyzed.

Scanning electron microscopy (SEM). The leaf samples were fixed overnight under vacuum in *Karnovsky Solution* (Morris 1965), composed of paraformaldehyde 4%, glutaraldehyde 0.5%, in sodium cacodylate buffer 0.1 M, pH7.2. Then, it was dehydrated in a graded acetone series (50–100%), critical-point dried with liquid CO_2, and finally fixed to aluminium SEM stubs, followed by a gold coating (Danilatos 1988). The analysis was performed using a Zeiss DSM 940A SEM (at NAP/MEPA –Piracicaba–USP). A total of 30 leaves of each point (pristine–PA_{P1}, PA_{P2}, and PA_{P3}; and disturbed–DA_{P1}, DA_{P2}, and DA_{P3}) were analyzed.

Comparing anatomical features: pristine vs. disturbed areas. The compared tissue biometry analysis was made in cross-sections of the leaves for the following features: thickness and diameter of the central rib (µm), thickness and diameter of the main vascular bundle (µm), mesophyll thickness (µm), hypodermis thickness (µm), palisade parenchyma thickness (µm), and both density of the stomata, and druse crystals (unity/µm^2). Each feature was analyzed in ten different sections, in 50 measurements per plant, through the Axion Vision (Zeiss) software. The quantification of the stomata was made through SEM images. The density of the epidermal structures was estimated in images with 1000 × magnification, in which it provided ten random fields (all in the abaxial face), for each sample. It allowed analyzing an area of 230.400 µm^2 of the foliar surface. The biometric and quantification data's similarities and differences were compared at each collection point; using the *t*-test ($\alpha = 95\%$).

Chemical analysis *Preparation of plant extracts*. A total of 100 fresh leaves of *C. criuva* from each sampling point (P_1, P_2, and P_3) were washed, lyophilized, powdered in a ball mill, and sieved through a #60 mesh. The powder (20 g) was macerated in an Erlenmeyer with 0.5 L ethanol: water (70% v:v) for seven days at room temperature (25 °C) and protected from light. The macerate was filtered in a Büchner funnel under vacuum (paper filter n° 1) and further concentrated until complete dryness using a Rotary evaporator at temperatures < 40 °C, under vacuum.

Clean-up of the extracts. As exposed by Soares et al. (2018), an aliquot (0.5 mg) of each *C. criuva* ethanolic extracts were individually solubilized in 2.0 mL methanol/ water (9:1, v/v) and applied onto a C18 cartridge (Strata C18-E, Phenomenex). The samples were eluted using methanol (100% v/v), and then filtered (Simplepure PTFE 0,22 µm, Allcrom) and diluted to around 5.0 mg.mL^{-1} in methanol/water (8:2, v/v).

Electrospray ionization mass spectrometry fingerprinting (FIA-ESI-IT-MS/MS). After solid-phase extraction, an aliquot of the extract was analyzed by flow injection analysis (FIA) using a LTQXL Thermo Finnigan Fisher (San Jose, CA, USA) mass spectrometer equipped with an electrospray ionization source (ESI), attached to an ion-trap (IT) analyzer. The ethanolic extracts obtained after clean-up (0.1 mg each) were diluted at 5 ppm using a methanolic solution 80% (v:v) with mass-grade methanol. The mass spectrometry analyses were adapted from (de Souza Mesquita et al. 2017, 2018; Tangerina et al. 2018). The negative ionization mode was chosen due to its superior effectiveness in ionizing the known biomarkers compounds compared to the positive mode. Subsequently, MS/MS analysis was conducted in the negative ionization mode with a flow rate of 5 µL/ min following the conditions: capillary voltage set at −4 V, spray voltage at 5 kV, tube lens offset at 75 V, capillary temperature at 280 °C, and sheath gas (N_2) flow rate at 60 arbitrary units. Mass spectra were recorded within the *m/z* range of 150–1500 Da. The first event was a full scan mass spectrum to acquire data on ions in the *m/z* range. The second scan event was an MS/MS experiment performed using a data-dependent scan on deprotonated molecules from the compounds at a collision energy of 20–30% and an activation time of 25–35 ms. All the compounds were proposed on the basis of their fragmentation patterns compared to the available literature data.

As described by de Andrade et al. (2018), the statistical data regarding the similarity index of the chemical composition from the PA and DA was exposed by multivariate analysis by multidimensional scaling (MDS), resulting in a similarity cluster, which was performed using the Jaccard coefficient of similarity, that reveals how similar the areas are in terms of shared chemical markers (compared between each other). A matrix of presence (+) and absence (−) of the chemical metabolites was constructed for each collection. For this, the *m/z* was the criterion for distinguishing each compound detected, previously identified according to the MS/MS fragmentations analysis and confirmed by the previous identification in the scientific literature. All multivariate analysis was conducted using Primer 6.0 software.

3 Results

Environmental contamination and anthropogenic pressures – The survey yielded 19 valid articles presenting contaminant data from samples obtained between 2002 and 2017. These results lead to 214 unique records based on several matrices such as sediment, biota samples, water, and pellets obtained along the coastal zones of nine cities in both regions North (Guarujá, Bertioga, Cubatão, São Vicente and Santos), around DA, and South (Juréia, Peruíbe, Iguape, and Cananéia), located around PA. A total of 114 records were based exclusively on sediment, 81 in biota samples, 16 on pellets, and three on water. Most records were from Cananéia (22%–43 records), Peruíbe (21%–40 records) and Santos (17%–32 records). Iguape, Cubatão, Juréia, São Vicente, Bertioga, and Guarujá represented together with the 40% remaining records.

In the Northern region, 58 records were based exclusively on sediment, 14 in biota samples (Crustacea and Mollusca), four in pellets, and two in water. Considering the entire dataset, sediment levels of non-essential (Cd, Pb, As, Hg, Al) and essential (Cu, Mn, Zn, Cr, Ni, Fe) metals ranged from zero to 1,743 to 710 mg/kg, respectively. In organisms, non-essential metal concentrations varied between zero to 2,269 mg/kg in Mollusca, and 10 to 309 mg/kg in Crustacea. Other contaminants such as the 16 priority Polycyclic Aromatic Hydrocarbons (PAHs) indicated by States Environmental Protection Agency (USEPA), Dichloro-diphenyl-trichloro-ethane (DDTs), and Polychlorinated biphenyl (PCBs) ranged between 88 to 2,068, zero to 130 and 336 to 451 ng/g, respectively (Fig. 2a, b).

In the Southern region, 56 records were based exclusively on sediment, 67 in biota samples (Crustacea and Actnopterigii), seven on pellets, and one on water. Considering the entire dataset, sediment levels of non-essential and essential metals ranged from 0.75 to 9,656 and zero to 3,842 mg/kg, respectively. Other contaminants, such as the 16 priority PAHs, DDTs, and PCBs ranged between 33 to 268, 11 to 55, and 81 to 163 ng/g, respectively. These levels are below the concentrations found in the northern region, which was expected in the PA since this site is a legally protected area with a small traditional community.

According to the non-essential metal analysis in sediment, the North region presented 16 records below ERL and

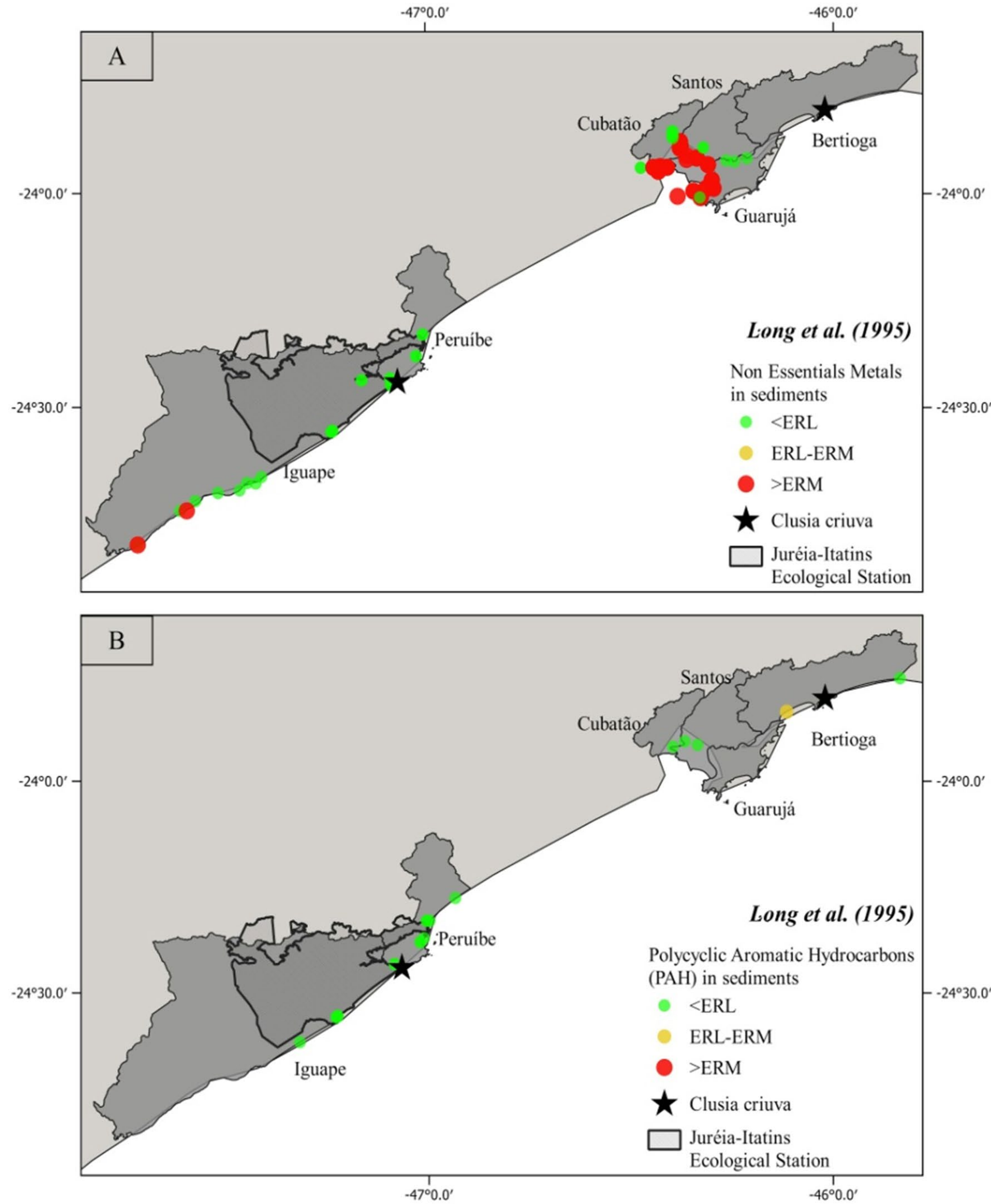

Fig. 2 Non-essential metals (**A**) and PAH (**B**) records between 2002 and 2017 in sediment samples distributed along PA and DA. The star points out to the region where *C. criuva* samples were collected

37 above ERM, meaning that most of the records (Fig. 2a) can affect organisms. On the other hand, the Southern region reported 38 records below ERL, one form between ERL and ERM, and 17 above ERM, mainly concentrated in the Cananéia estuary. According to year variations, this harmful concentration in the region can be related to the internal circulation on the Southeastern coast, as explored by (Moreira et al. 2016).

Anatomical analysis – The analysis of the foliar anatomic structure both from PA and DA have similar qualitative features (Fig. 3). The foliar anatomy is characterized by a thick

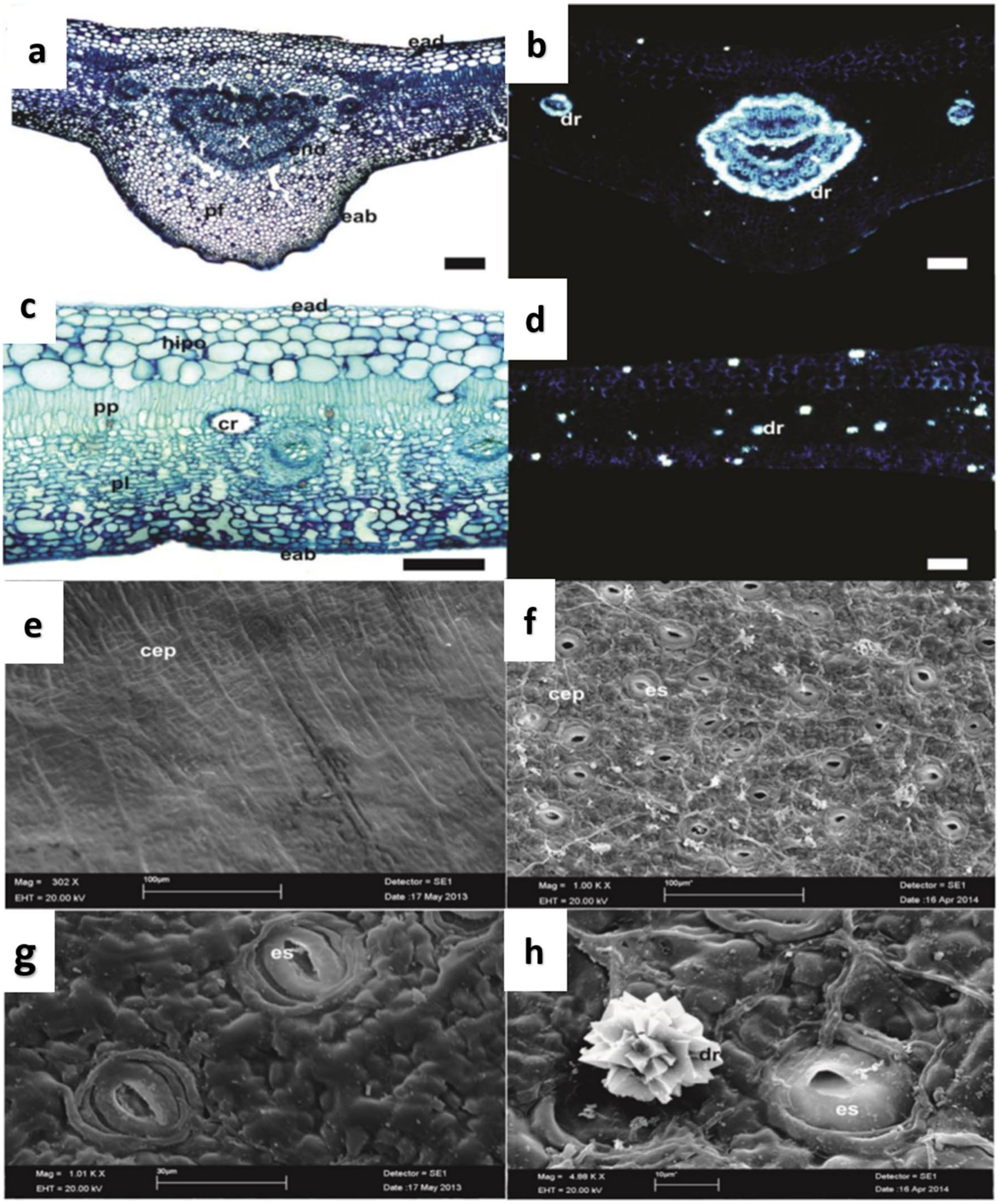

Fig. 3 Anatomical features of *Clusia criuva* leaves from PA (**a**, **b**, **d**, **h**) and DA (**c**, **e**, **f**, **g**). **a**, **b** Midrib in cross-section, under light and polarized light microscopy, respectively. **c**, **d** Foliar blade in cross-section, under light and light polarized microscopy, respectively. **e** SEM of the adaxial surface. **f** SEM of the abaxial surface. **g**, **h** Detail of the stomata, and cuticle microrelief. cep: epicuticular wax, cr: resiniferous channel, dr: druse, eab: abaxial epidermis surface; ead: epidermis adaxial surface; end: endodermis, es: stomata, f: floem, hipo: hypodermis, pl: lacunary parenchyma pp: palisade parenchyma, st: stomata, x: xylem, Bars: 10×/scale 100 µm (**a**, **b**, **d**); 20×/scale 50 µm (**c**), 100 µm (**e**, **f**) 30µ (**g**), 10 µm (**h**)

cuticle in the adaxial and abaxial epidermal foliar faces; however, it is even thicker on the adaxial one. The heterogeneous mesophyll exhibits hypodermis with 5–6 cellular layers in the adaxial side (Fig. 3a, c); 1–2 layers of palisade parenchyma, and 16–19 layers of spongy parenchyma (Fig. 3a, c); and resiniferous channels between the palisade and spongy parenchyma (Fig. 3a, c). There are dense central vascular bundles surrounded by endodermis (Fig. 3a). The central rib is plain-convex, *i.e.*, with a prominence in the abaxial face, exhibiting a collateral vascular bundle (Fig. 3a). Under polarized light analysis, a multiple lignification process (Fig. 3b, d), and several druse crystals (Fig. 3b, d), are also highlighted in Fig. 3h by an SEM image. The paracytic stomata (Fig. 3f, g) occur on the abaxial face, inside crypts, showing large substomatal chambers, characterizing the leaf of *C. criuva* as hypostomatous type (Fig. 3c). Thus, we selected nine anatomic features to evaluate their quantitative modifications to proceed with the biometry analysis (Fig. 4). Plants from the PA have a thicker foliar area than leaves from the DA. Namely expressed by the central rib thickness (µm), central vascular bundle thickness (µm), the diameter of the vascular bundle (µm), mesophyll thickness (µm), hypoderms thickness (µm), and palisade parenchyma thickness (µm) (*t*-test: $p < 0.05$). In contrast, the druse density (druses/µm^2) was higher in plants from the DA. Both central rib diameter (µm), and stomata density (stomata/µm^2) showed no significant difference between the PA, and DA (*t*-test: $p > 0.05$).

Chemical analysis – A total of 12 chemical compounds were identified by FIA-ESI-IT-MS/MS (Table 1) from the extracts of *C. criuva* leaves. These compounds were classified into three main classes: flavonoids [catechin trimer (*m/z* 865), cirsiliol-dihexoside (*m/z* 653), vitexin-hexoside (*m/z* 593), vitexin-deoxyhexoside (*m/z* 577), apigenin-hexoside-pentoside (563), catechin derivative (*m/z* 455), isoorientin/orientin (*m/z* 447), vitexin (*m/z* 431)]; benzophenones, namely the 7-*epi*-nemorosone (*m/z* 501); and phenolic acids (acetyldicaffeoylquinic acid (*m/z* 557), caffeoylquinic acid (*m/z* 353), and quinic acid (*m/z* 191)].

Several known flavonoids and glycosyl derivatives were identified in PA and DA samples. To obtain qualitative information about the compounds present in *C. criuva* extracts, a total scan mass spectrometry fingerprinting was obtained in negative mode, showing the $[M\text{-}H]^-$ adduct ions. Six different flavonoid aglycones and their derivatives were detected, including catechin, cirsiliol, vitexin, apigenin, and isoorientin/orientin. Catechin derivatives (*m/z* 865, 455) were detected in samples from the DA (Table 1, ID 1, and 8), leading to a final ion at *m/z* 289 (catechin moiety). The MS^2 spectrum of ion *m/z* 865 produced a major fragment at *m/z* 577 $[M\text{-}288\text{-}H]^-$ arose from the loss of a catechin moiety, typical fragmentation of catechin derivatives, described as a quinone methide (QM). The MS^3 fragmentation of the ion

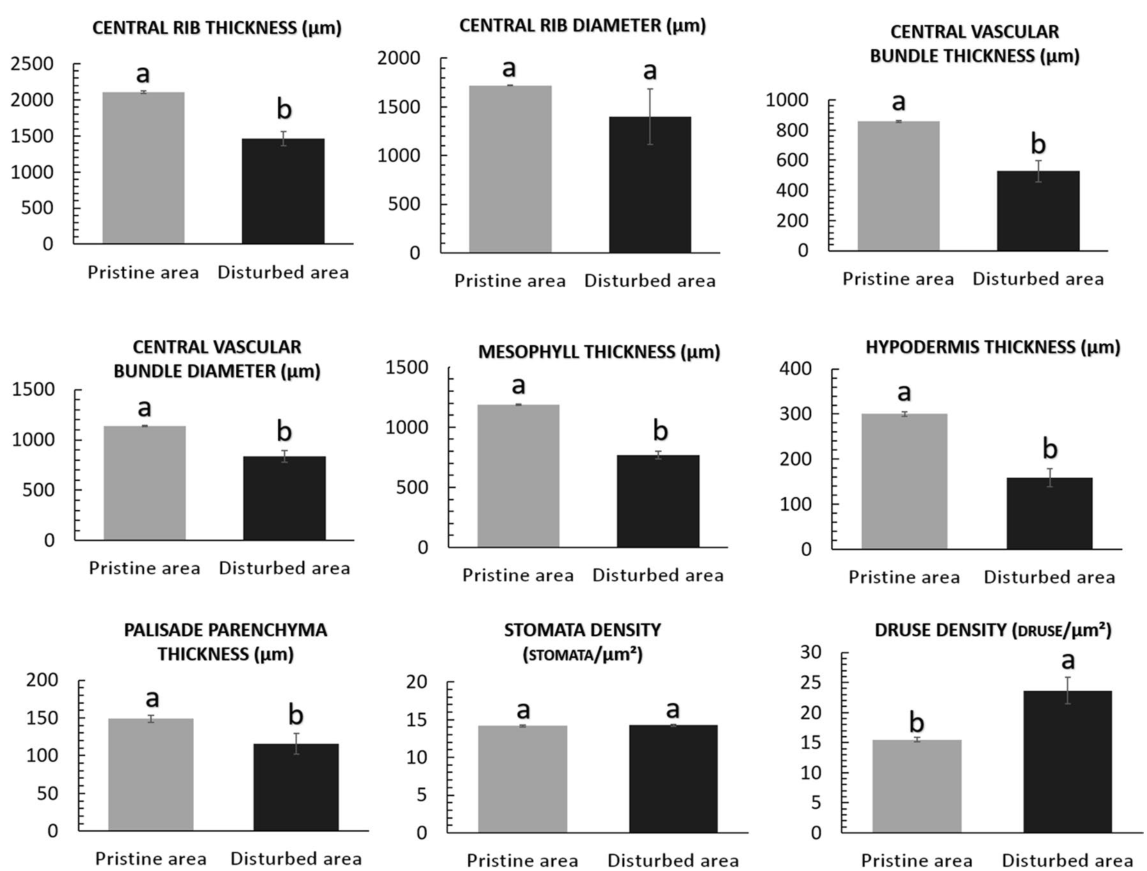

Fig. 4 Comparison of the anatomical features regarding the quantitative parameters from Pristine area (PA) and Disturbed area (DA)

Table 1 A*m/z* [M–H]- ion of markers characterized in both areas (pristine area—PA and disturbed area—DA); Fragments of the molecules obtained by FIA-ESI-IT-MS/MS of the ethanolic extract from *Clusia criuva* leaves for each sample, namely PA (PA_{P1},PA_{P2},PA_{P3}), DA (DA_{P1},DA_{P2}, and DA_{P3})

ID	Compounds	*m/z* [M-H]⁻	MS/MS	Pristine (PA)			Disturbed (DA)			References
				Sampling points						
				PA_{P1}	PA_{P2}	PA_{P3}	DA_{P1}	DA_{P2}	DA_{P3}	
1	Catechin trimer	865	MS^2: 577 $[M\text{-}288\text{-}H]^-$ MS^3: 451 $[M\text{-}126\text{-}H]^-$, 425 $[M\text{-}152\text{-}H]^-$, 289 $[M\text{-}288\text{-}H]^-$	–	–	–	+	+	–	de Souza Mesquita et al. (2018)
2	Cirsiliol-dihexoside	653	MS^2: 635, 491 $[M\text{-}162\text{-}H]^-$, 447, 329	+	+	+89	+	–	+	Biazotto et al. (2019)
3	Vitexin-hexoside	593	MS^2: 473 $[M\text{-}120\text{-}H]^-$, 413 $[M\text{-}180\text{-}H]^-$	+	+	+	+	+	+	Iwashina et al. (2015)
4	Vitexin-deoxyhexoside	577	MS^2: 457 $[M\text{-}120\text{-}H]^-$, 431 $[M\text{-}146\text{-}H]^-$, 413 $[M\text{-}146\text{–}18\text{-}H]^-$, 293 $[M\text{-}284\text{-}H]^-$	–	–	–	+	+	+	Iwashina et al. (2015)
5	Apigenin + hexoside + pentoside	563	MS^2: 443 $[M\text{-}120\text{-}H]^-$, 383$[M\text{-}180\text{-}H]^-$, 353 MS^3: 269 $[M\text{-}162\text{–}132\text{-}H]^-$	+	–	+	+	+	+	Benayad et al. (2014)
6	Acetyl-dicaffeoyl quinic acid	557	MS^2: 395 $[M\text{-}162\text{-}H]^-$, 377 $[M\text{-}180\text{-}H]^-$, 353, 233 MS^3: 335, 233 $[M\text{-}162\text{-}H]^-$, 191, 173	+	+	+	–	–	–	Zhang et al. (2007)
7	7-epi-nemorosone	501	MS^2: 432 $[M\text{-}69\text{-}H]^-$, 363 $[M\text{-}138\text{-}H]^-$, 309 $[M\text{-}192\text{-}H]^-$	–	–	–	+	+	+	Anholeti et al. (2015)
8	Catechin derivative	455	289 $[M\text{-}166\text{-}H]^-$, 193 $[M\text{-}262\text{-}H]^-$	–	–	–	+	+	–	Dou et al. (2007)
9	Isoorientin/Orientin	447	MS^2: 357 $[M\text{-}90\text{-}H]^-$, 327$[M\text{-}120\text{-}H]^-$, 311, 297, 285	+	–	–	+	+	+	Chen et al. (2016)
10	vitexinV Vitexin	431	415 $[M\text{-}16\text{-}H]^-$, 397, 379 $[M\text{-}90\text{-}H]^-$, 367, 351 $[M\text{-}80\text{-}H]^-$, 269 $[M\text{-}162\text{-}H]^-$	+	+	+	+	+	+	Iwashina et al. (2015)
11	Caffeoyl-quinic acid	353	MS^2 191 $[M\text{-}162\text{-}H]^-$, 179	+	+	+	–	–	–	de Souza Mesquita et al. (2018)
12	Quinic acid	191	MS^2 172,163,110	+	+	+	–	–	–	de Souza Mesquita et al. (2018)

"+" = presence of the compound; "–" = absence of the compound *m/z* 865 showed major fragments at *m/z* 451 [M-126-H]$^-$, 425 [M-152-H]$^-$, and 289 [M-288-H]$^-$, which represents a typical fragmentation pathway of catechin derivatives, denominated as a subsequent QM-fragmentation, retro-diels–alder [M-152-H]$^-$, and heterocyclic ring fission [M-126-H]$^-$. The second class of flavonoids was also detected in *C. criuva* extracts, the flavone cirsiliol-dihexoside (*m/z* 653) (Table 1, ID 2), which was detected in both areas (PA and DA), the MS^2 spectrum of the ion at *m/z* 653 lead to major fragments at 491 [M-162-H]$^-$ (hexose moiety), and 329 (cirsiliol aglycone after a sequential loss of a second hexoside moiety. As a third class, the apigenin derivatives, vitexin/isovitexin (*m/z* 431) was also detected (Table 1, ID 10). Vitexin derivatives have shown typical fragmentations of *c*-glycoside compounds, evidenced by [M-120-H]$^-$, [M-90-H]$^-$, and [M-180-H]$^-$, and the same final product at *m/z* 431. Vitexin-deoxyhexoside (*m/z* 577) (Table 1, ID 6) was detected only in samples from DA, unlike vitexin-hexoside (*m/z* 593) (Table 1, ID 3), and vitexin aglycone (*m/z* 269), which are present in samples from both areas (PA and DA). In addition, the apigenin glycoside (*m/z* 269) was detected in both areas, evidenced by the MS^2 spectrum of the ion at *m/z* 563, which led to fragmentations of hexoside + pentoside moieties [M-162–132-H], suggesting an apigenin-hexoside-pentoside compound (Table 1, ID 5). Isoorientin/orientin glycosides (*m/z* 447, Table 1, ID 9) were also detected in *C. criuva* extracts (DA_{P1}, DA_{P2}, and DA_{P3}, and in the PA_{P1}).

The second class of compounds (phenolic acids) could also assist the purpose of *C. criuva* as a bioindicator since quinic acid derivatives (*m/z* 191) are only found in samples from PA (Table 1, ID 6, 11, and 12). According to the MS^2 spectrum of these compounds, a common fragmentation pathway, such as 557 → 443 [M-162-H] $^-$, and 557 → 353 [M-162–42-H]$^-$ are observed, leading to the final primary ion at *m/z* 191, which also is observed in the MS^2 spectrum of the ion *m/z* 353[M-162-H]$^-$. In contrast, the benzophenone here identified as 7-*epi*-nemorosone (Table 1, ID 7) was only detected in samples from DA. The MS^2 of the ion *m/z* 501 leads to the classical fragmentation of 69 Da, representing a loss of an isoprene moiety.

Subsequently, the mass spectrometry data (Table 1) was analyzed, and multivariate analysis was conducted and depicted as cluster and multidimensional scaling (MDS) plots (Fig. 5). The results yielded two significant observations. Firstly, a low similarity index (40%) indicated a notable difference in the chemical composition of PA and DA samples (Fig. 5a; Table S1 – supplementary material). Secondly, samples of *Clusia* collected from the same area, when compared with each other (PA-PA and DA-DA), exhibited a high similarity index (≥ 80%). This was further emphasized in the MDS plot (Fig. 5b), which clearly displayed two distinct groups with a low similarity index between them. These findings suggest that the chemical composition of *C. criuva* holds potential as a bioindicator model, as it demonstrates evident variations in composition between different areas and strong consistency within the same area.

4 Discussion

This study takes an integrative approach to examine the chemical and anatomical characteristics of *C. criuva* leaves as a potential indicator of disturbances in coastal vegetation caused by high levels of human activity. Previous studies have shown that environmental factors, including climate and contamination, can significantly affect plant species' chemical composition and morpho-anatomical features (Olsen et al. 2013; Rahman et al. 2023), including in the *Clusia* genus (da Silva et al. 2005, 2017b). Moreover, leaves are more sensitive to air pollutants than other plant organs like stems and roots (Gostin 2009). Therefore, this research comprehensively analyses *C. criuva* as a potential bioindicator of anthropization, given its resilience in coastal plain ecosystems (Caris et al. 2013).

The differences in anatomical and chemical characteristics found in *Clusia leaves* from polluted and pristine areas may be related to potential exposure to pollutants and anthropogenic pressures. The coastal zone has undergone intense landscape modifications resulting in habitat degradation of Restinga areas (Rocha et al. 2007). This process is associated with intense urbanization and seasonal pressures due to tourism, industrial, and harbor activities, including the potential transport of contamination from the Bertioga Channel, considering the prevailing currents along the coast. The data presented here highlight the significant impact of anthropization in the DA area, primarily attributed to pollutants originating from nearby industries and the adjacent harbor complex. Moreover, human sewage and fuel contamination from crafts and boat marinas, which are not continuously present in the pristine area (PA), may also impact the development of organisms in coastal ecosystems and the dynamics of the natural environment. In contrast, the anthropization, contamination, and tourism levels in the PA, located in Peruíbe/Iguape, are negligible compared to the entire São Paulo state. Therefore, despite collecting the samples from the terrestrial area, all these factors might have influenced the findings. Indeed, while our data do not establish a direct correlation between anthropization factors and the observed differences in characteristics between the two areas, the presented data strongly suggests that these differences are attributable to anthropization. This conclusion is supported by a comprehensive literature review that thoroughly characterizes the anthropization factors in both areas. The climate conditions in both DA and PA, including

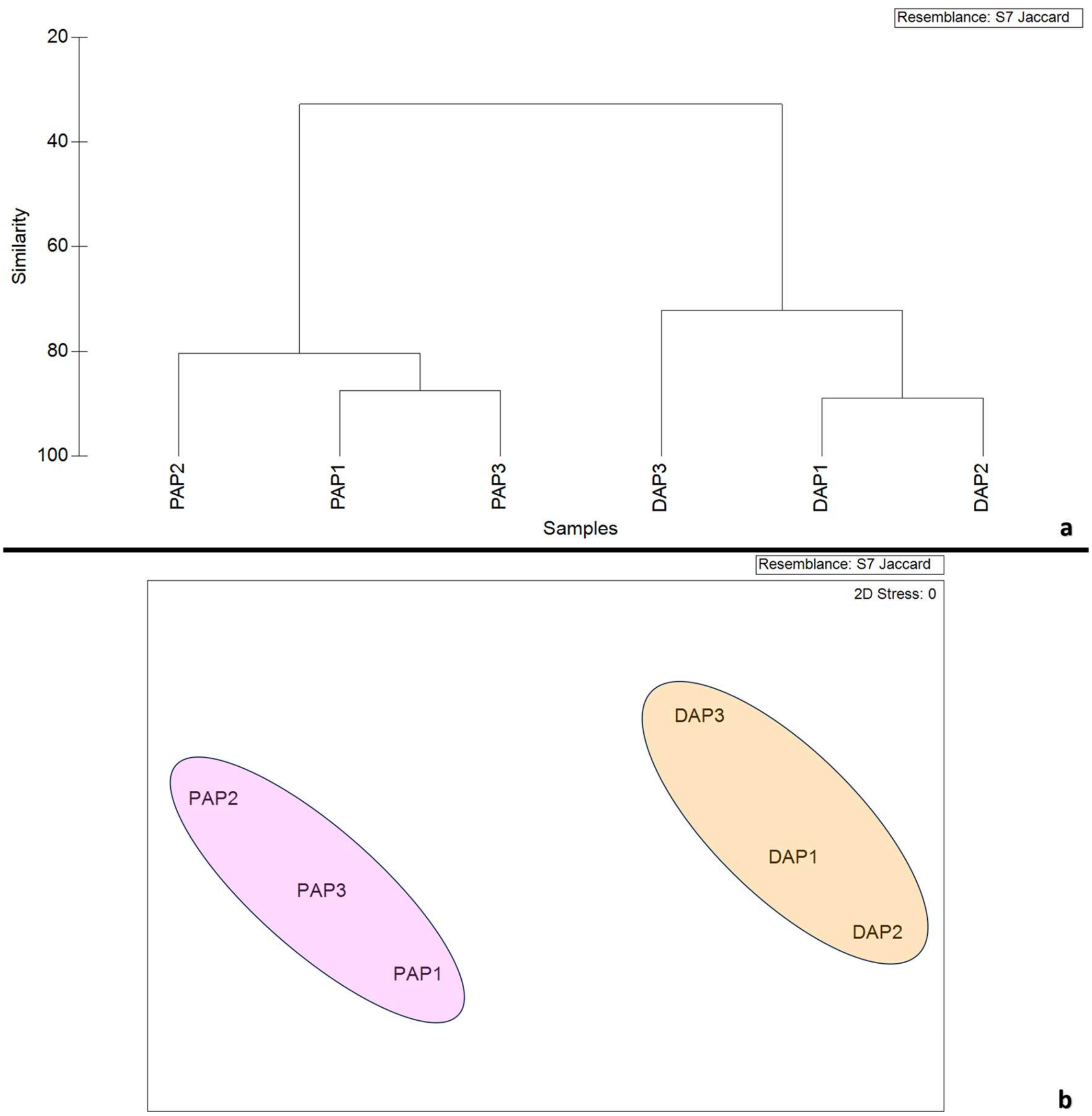

Fig. 5 **a** Cluster and **b** MDS plots representing the chemical similarity between Pristine area (PA) and Disturbed area (DA). DA_{P1}, DA_{P2}, and DA_{P3} represent the different sampling points from DA (Bertioga); PA_{P1},PA_{P2}, and PA_{P3} represent the different sampling points from PA (Iguape/Peruíbe)

temperature amplitude and rainfall regimes, are similar. Both areas are located near the shoreline in sandy coastal ecosystems known as resting. However, there are notable differences between the two areas regarding contamination levels and human presence, reinforcing the possible explanation we exposed.

Besides, although the São Lourenço area in Bertioga (DA) is not considered to be heavily polluted, it may still be vulnerable to exposure to contaminants that are dispersed through water, such as plastic pellets containing adsorbed organic pollutants and PAHs (Fig. 2b), which can reach the beach area, as previously demonstrated (Taniguchi et al. 2016). Additionally, the presence of an important industrial centre (Cubatão Industrial Complex), the largest port in Brazil (Port of Santos), and the largest oil terminal (Almirante Barroso Maritime Terminal) in Latin America contribute considerably to the input of organic contaminants, such as PAHs, DDT, and PCBs, into the marine and coastal environment near DA (Abessa et al. 2005; Fisner et al. 2013; Taniguchi et al. 2016). Furthermore, it is established that certain plant species exhibit sensitivity towards pollutants present in the atmosphere, soil, and water and may display stress responses upon exposure, making them valuable as bioindicators (Neves et al. 2009; Siqueira-Silva et al. 2012), including *C. hilariana* (da Silva et al. 2017b). Thus, considering the proximity of the Riviera de São Lourenço area (DA) to the industrial complex of Cubatão and the densely urbanized region in its surroundings (Baixada Santista), it is plausible that the local vegetation may encounter atmospheric pollutants emanating from these anthropogenic sources.

The observed xerophytic foliar pattern in both PA and DA areas reveals the physiological stress caused by limited water and nutrient availability due to the halophile-sandy soil of the ecosystem. However, there were no discernible qualitative differences between the areas. The region is known for its heavily impacted mangrove area and being home to one of Brazil's largest industrial centres, Cubatão City (Banci et al. 2017). Despite some values falling below acceptable levels, organic compounds and other contaminants in this Northern coastal region suggest anthropogenic interference (Abessa et al. 2017). Studies assessing levels of toxic metals in Santos and São Vicente Bay suggest that local biota may be adversely affected by sewage discharge and urban drainage (Araujo et al. 2013). Furthermore, marine currents flow towards the north, resulting in high disposal of organic matter and contaminants from Santos Bay to adjacent open areas (Braga et al. 2000), such as Guarujá and Bertioga Coasts.

Regarding the anatomical features, our findings support previous studies indicating that *C. criuva* exhibits xerophytic traits in response to the halophile-sandy soil and limited water and nutrients in the coastal ecosystem. These traits include a thick cuticle, hypodermis with large cells, double palisade parenchyma, stomatal crypts, and abundant druses (Boeger and Wisniewski 2003; Barrera Zambrano et al. 2014; Banci et al. 2017; da Silva et al. 2017a). It is already known that leaves from polluted areas have been found to have a higher density of calcium oxalate crystals, such as druses, particularly in regions with high human density, air pollution, and heavy metal contamination (Tomašević et al. 2008; Gostin 2016). These findings align with our own research, revealing a significant disparity in the density of druse crystals. Specifically, the DA area exhibited an approximately twofold higher density of druses than the PA area. Besides, the anatomical parameters indicate that thickness parameters such as the central rib, central vascular bundle, mesophyll, and hypodermis are higher in plants from the PA area. This suggests that plants in PA are exposed to more intense UV solar radiation compared to those in DA. Plants can modulate their thickness in response to UV radiation exposure. This adaptive mechanism enables them to mitigate the loss and denaturation of vital nutrients within leaf tissues (Mao et al. 2018). Thus, the main possible explanation to it is the disparity may be attributed to the shading effects caused by air follicular pollution in the DA area. As depicted in Fig. 1, the wind direction of the industrial complex from Cubatao carries pollution towards Bertioga—DA. Furthermore, these findings align with the results reported by da Silva et al. (2017a, b), who concluded that C. hilariana serves as an effective bioindicator of atmospheric pollutants emitted by the pelletizing factory. Their study revealed distinct damage patterns in the vegetation surrounding the factory, providing valuable insights into the types and effects of atmospheric pollutants on the local plant life. Therefore, taking into account the existing evidence suggesting the effectiveness of *Clusia* species as reliable bioindicators of a large plethora of air pollutants and considering that the DA area is subjected to a complex multilevel pollutant zone, our findings provide valuable information regarding the potential use of native *Clusia criuva* plants as promising bioindicators in restingas.

Several studies have reported that secondary metabolites are crucial in plant defense and can be helpful as natural products (Divekar et al. 2022). However, the production of these compounds is strongly influenced by various environmental factors such as temperature, light, soil water, nutrient availability, salinity, and contamination (Yang et al. 2018). Thus, regarding the chemical composition of the leaves collected in DA and PA, the MDS and cluster plots could be a valuable tool to differentiate pristine and disturbed areas from *Restinga* ecosystems. Indeed, the identified compounds have been previously identified in *Clusia* species and are known to act as chemotaxonomic markers, mainly vitexin derivatives and 7-*epi*-nemerosone (Compagnone et al. 2008; Piccinelli et al. 2009; Anholeti et al. 2015). Although notable differences were observed in the secondary metabolites between the DA and PA, establishing a direct link between the chemical composition of each extract and the level of anthropization or contamination in their respective environments remains challenging. However, it is worth noting an intriguing finding: the exclusive presence of a common chemical marker of the *Clusia* genus, 7-*epi*-nemerosone, in the DA area. In contrast, even quinic acid derivatives being commonly found in various plant species, were only detected in the extracts of *C. criuva* collected from the PA. This observation suggests a potential association with specific biosynthetic pathways unique to each class of compounds.

Isoprenes and quinic acids are synthesized through distinct biosynthetic pathways. Isoprenes are derived from either the mevalonate pathway or the methylerythritol phosphate (MEP) pathway (Skorupinska-Tudek et al. 2008), while quinic acids are synthesized via the shikimate biosynthesis pathway (Lallemand et al. 2012). These pathways represent two separate synthetic routes in plants. When it comes to plant defense, comparing the effectiveness of isoprenes and quinic acids directly is challenging due to their different modes of action. Both compounds contribute to the overall defense system of plants, but their specific roles and efficacy can vary depending on factors such as plant species, environmental conditions, and the specific challenges the plant faces.

Due to their conjugated double-bounds, isoprenes possess more substantial antioxidant properties than quinic acids derivatives (especially compared to those glucosilated), which can aid in protecting plant tissues from oxidative damage. In the case of the specimens collected in the DA, they are exposed to a high multilevel oxidative stress. This oxidative stress is primarily attributed to heavy metals, PAHs, DDTs, and PCBs in significant quantities within and around the studied area. On the other hand, quinic acids and their derivatives are known for their role in plant defense against natural herbivores. They possess astringent and antifeedant properties, which can help protect plant tissues from herbivory. These findings align with a recent study that concluded that plants exhibiting a high content of quinic acid derivatives, as identified through a metabolomic approach, display resistance to herbivores, particularly insects (Leiss et al. 2009). Quinic acid derivatives in these plants likely contribute to their defensive mechanisms, deterring herbivory and enhancing their resilience against insect damage. This highlights the critical role of quinic acid derivatives in plant defense strategies and their potential significance in promoting plant resistance to herbivorous insects, which could be a reasonable justification for the data found in this study, considering that quinic acid derivatives were only detected in PA.

Based on the collected data regarding the chemical composition of specimens from the DA and PA areas, it is evident that there is a significant difference (> 50%) in the chemical profiles between the two areas. While the exact reasons for this difference are yet to be determined, it is plausible to consider that the disparity could be associated with the level of anthropization in each environment. However, further research and investigation are necessary to establish a direct link between the observed chemical differences and the degree of anthropization in the respective areas.

Pristine and polluted areas were successfully differentiated through the literature review and guidelines analysis, showing the presence of contaminants. However, DA presented nearly 70% of the records above ERM, in contrast to only 30% in PA, which may imply higher threats to local biodiversity in DA. Furthermore, this study recorded some significant changes in the anatomical features (mainly regarding the quantitative parameters) and the chemical composition of leaves from *C. criuva* between two areas (PA and DA), suggesting the potential effects of environmental contamination and disturbances in this *Restinga* species. From the structural point of view, the feature related to the thickness of the central rib central vascular bundle, mesophyll, hypodermis, and palisade parenchyma, along with the druse density, seems good environmental indicators for disturbed areas, in with the mesophyll and central rib are thicker in plants from PA, while the druse density was higher in plants from DA. Also, the chemical profile between these two studied areas indicated that quinic acid derivatives (ID 6, 11, 12) are found in plants from PA, which may be a response against intense herbivory agents. At the same time, 7-*epi*-nemerosone (ID **7**), a standard chemotaxonomic marker, was detected only in *C. criuva* that grows in DA, probably due to the need to defend the plant against oxidative stressors. Finally, our results may evidence a stress response to the plant exposed to contaminants and suggest the potential use of *C. criuva* as a bioindicator species for the environmental quality evaluation and monitoring of *Restinga* forests. Thus, since *Restinga* forests are poorly studied ecosystems and highly impacted by human pressures, we recommend future studies to investigate the impacts of specific anthropogenic stressors and understand their effects on the biodiversity of these environments. Further, this work may represent a model of the integrative method, considering a set of data (such as ecological, chemical, and botanical features) instead of a single feature to predict the environmental status of the region. Such an integrative approach may guarantee a more holistic response, which can promote conservation strategies for *Restinga* ecosystems, mainly regarding local authorities' decision-making and policies.

Supplementary Information The online version contains supplementary material available at https://doi.org/10.1007/s40415-023-00937-1.

Acknowledgements This work was supported by "Fundação de Amparo à Pesquisa do Estado de São Paulo–FAPESP" for funding's (2009/52237-9) and fellowship (LMSM–2011/23113-0; VFFP–2012/22899-2; CQR–2013/06188-1). WV also acknowledgements his CNPq grant (301397/2017-1).

Author contributions LMSM, VFFP, BZN, MNR and MPT conceived and designed the study. LMSM, VFFP, MNR, MPT and OJGA performed material preparation. LMSM, and VFFP completed experiments. All the authors conducted data analysis. The first draft of the manuscript was written LMSM, and afterwards completed by VFFP, BZN and CQR. LMSM, MBGM and WV performed the coordination of the research. All the authors read and approved the final manuscript.

Declarations

Conflict of interest The authors declare that they have no known competing financial interests or personal relationships that could have influenced the work reported in this paper.

References

Abessa DMS, Carr RS, Rachid BRF et al (2005) Influence of a Brazilian sewage outfall on the toxicity and contamination of adjacent sediments. Mar Pollut Bull 50:875–885. https://doi.org/10.1016/j.marpolbul.2005.02.034

Abessa D, Vicente TM, Moreira LB et al (2017) Assessing the sediment quality of the Laje de Santos marine state park and other marine protected areas of the central coast of São Paulo (Brazil). Braz J Oceanogr 65:532–548. https://doi.org/10.1590/s1679-87592017128606504

Anholeti MC, de Paiva SR, Figueiredo MR, Kaplan MAC (2015) Chemosystematic aspects of polyisoprenylated benzophenones from the genus Clusia. An Acad Bras Cienc 87:289–301. https://doi.org/10.1590/0001-3765201520140564

Araujo GS, Moreira LB, Morais RD et al (2013) Ecotoxicological assessment of sediments from an urban marine protected area (Xixová-Japuí State Park, SP, Brazil). Mar Pollut Bull 75:62–68. https://doi.org/10.1016/j.marpolbul.2013.08.005

Azzazy MF (2020) Plant bioindicators of pollution in Sadat City, Western Nile Delta. Egypt. Plos One 15:e0226315. https://doi.org/10.1371/journal.pone.0226315

Babaei F, Moafizad A, Darvishvand Z et al (2020) Review of the effects of vitexin in oxidative stress-related diseases. Food Sci Nutr 8:2569–2580. https://doi.org/10.1002/fsn3.1567

Barrera Zambrano VA, Lawson T, Olmos E et al (2014) Leaf anatomical traits which accommodate the facultative engagement of crassulacean acid metabolism in tropical trees of the genus Clusia. J Exp Bot 65:3513–3523. https://doi.org/10.1093/jxb/eru022

Benayad Z, Gómez-Cordovés C, Es-Safi NE (2014) Characterization of flavonoid glycosides from fenugreek (Trigonella foenum-graecum) crude seeds by HPLC–DAD–ESI/MS analysis. Int J Mol Sci 15:20668–20685

Biazotto KR, de Souza Mesquita LM, Neves BV et al (2019) Brazilian biodiversity fruits: discovering bioactive compounds from underexplored sources. J Agric Food Chem 67:1860–1876. https://doi.org/10.1021/acs.jafc.8b05815

Boeger MRT, Wisniewski C (2003) Comparação da morfologia foliar de espécies arbóreas de três estádios sucessionais distintos de floresta ombrófila densa (Floresta Atlântica) no Sul do Brasil. Rev Bras Botânica 26:61–72. https://doi.org/10.1590/S0100-84042003000100007

Braga ES, Bonetti CVD, Burone L, Bonetti Filho J (2000) Eutrophication and bacterial pollution caused by industrial and domestic wastes at the baixada santista estuarine system–Brazil. Mar Pollut Bull 40:165–173. https://doi.org/10.1016/S0025-326X(99)00199-X

Caris EAP, Kurtz BC, Cruz CBM, Scarano FR (2013) Vegetation cover and land use of a protected coastal area and its surroundings, southeast Brazil. Rodriguésia 64:747–755. https://doi.org/10.1590/S2175-78602013000400006

Chen G, Li X, Saleri F, Guo M (2016) Analysis of flavonoids in rhamnus davurica and its antiproliferative activities. Molecules 21:1275. https://doi.org/10.3390/molecules21101275

Compagnone RS, Suarez AC, Leitao SG, Delle Monache F (2008) Flavonoids, benzophenones and a new euphane derivative from Clusia columnaris Engl. Rev Bras Farmacogn 18:6–10. https://doi.org/10.1590/S0102-695X2008000100003

Cruz ACF, Gusso-Choueri P, de Araujo GS et al (2019) Levels of metals and toxicity in sediments from a Ramsar site influenced by former mining activities. Ecotoxicol Environ Saf 171:162–172. https://doi.org/10.1016/j.ecoenv.2018.12.088

da Banci KRS, Mori GM, de Oliveira MA et al (2017) Can environmental pollution by metals change genetic diversity? Ucides cordatus (Linnaeus, 1763) as a study case in Southeastern Brazilian mangroves. Mar Pollut Bull 116:440–447. https://doi.org/10.1016/j.marpolbul.2017.01.039

da Silva LC, Oliva MA, Azevedo AA et al (2005) Micromorphological and anatomical alterations caused by simulated acid rain in Restinga plants: Eugenia uniflora and Clusia hilariana. Water Air Soil Pollut 168:129–143. https://doi.org/10.1007/s11270-005-0941-2

da Silva LC, de Araújo TO, Martinez CA et al (2015) Differential responses of C3 and CAM native Brazilian plant species to a SO2- and SPMFe-contaminated Restinga. Environ Sci Pollut Res 22:14007–14017. https://doi.org/10.1007/s11356-015-4391-0

da Silva KMM, da Nóbrega AB, Lessa B et al (2017a) Clusia criuva Cambess. (Clusiaceae): anatomical characterization, chemical prospecting and antioxidant activity. An Acad Bras Cienc 89:1565–1578. https://doi.org/10.1590/0001-3765201720160286

da Silva LC, de Araújo TO, Siqueira-Silva AI et al (2017b) Clusia hilariana and Eugenia uniflora as bioindicators of atmospheric pollutants emitted by an iron pelletizing factory in Brazil. Environ Sci Pollut Res 24:28026–28035. https://doi.org/10.1007/s11356-017-0386-3

Danilatos GD (1988) Foundations of environmental scanning electron microscopy. Advances in electronics and electron physics. Elsevier, Amsterdam, pp 109–250

de Andrade CG, de Souza Mesquita LM, Murador DC et al (2018) Application of electrospray ionization mass spectrometry fingerprinting associated with macroscopic and histological analysis for Plantago major herbal infusions quality control. Food Res Int 107:314–324. https://doi.org/10.1016/j.foodres.2018.02.031

de Duarte LFA, Moreno JB, Catharino MGM et al (2019) Mangrove metal pollution induces biological tolerance to Cd on a crab sentinel species subpopulation. Sci Total Environ 687:768–779. https://doi.org/10.1016/j.scitotenv.2019.06.039

de Souza ML, Caria C, Santos P et al (2018) Modulatory effect of polyphenolic compounds from the mangrove tree rhizophora mangle L. on non-alcoholic fatty liver disease and insulin resistance in high-fat diet obese mice. Molecules 23:2114. https://doi.org/10.3390/molecules23092114

de Souza Mesquita LM, Colpo KD, da Rocha CQ et al (2017) Anatomical differentiation and metabolomic profiling: a tool in the diagnostic characterization of some medicinal Plantago species. Brazilian J Bot 40:801–810. https://doi.org/10.1007/s40415-017-0388-x

Defeo O, McLachlan A, Schoeman DS et al (2009) Threats to sandy beach ecosystems: a review. Estuar Coast Shelf Sci 81:1–12. https://doi.org/10.1016/j.ecss.2008.09.022

Divekar PA, Narayana S, Divekar BA et al (2022) Plant secondary metabolites as defense tools against herbivores for sustainable crop protection. Int J Mol Sci 23:2690. https://doi.org/10.3390/ijms23052690

Dou J, Lee VSY, Tzen JTC, Lee M-R (2007) Identification and comparison of phenolic compounds in the preparation of oolong tea manufactured by semifermentation and drying processes. J Agric Food Chem 55:7462–7468

Fisner M, Taniguchi S, Majer AP et al (2013) Concentration and composition of polycyclic aromatic hydrocarbons (PAHs) in plastic pellets: implications for small-scale diagnostic and environmental monitoring. Mar Pollut Bull 76:349–354. https://doi.org/10.1016/j.marpolbul.2013.09.045

Gostin IN (2009) Air pollution effects on the leaf structure of some Fabaceae species. Not Bot Horti Agrobot Cluj Napoca 37:57–63. https://doi.org/10.15835/nbha3723078

Gostin I (2016) Air pollution stress and plant response. Plant responses to air pollution. Springer Singapore, Singapore, pp 99–117

Gustafsson MHG, Bittrich V, Stevens PF (2002) Phylogeny of clusiaceae based on rbc L sequences. Int J Plant Sci 163:1045–1054. https://doi.org/10.1086/342521

Gustafsson MHG, Winter K, Bittrich V (2007) Diversity, phylogeny and classification of clusia. Clusia. Springer, Berlin Heidelberg, pp 95–116

Harris L, Nel R, Holness S, Schoeman D (2015) Quantifying cumulative threats to sandy beach ecosystems: A tool to guide ecosystem-based management beyond coastal reserves. Ocean Coast Manag 110:12–24. https://doi.org/10.1016/j.ocecoaman.2015.03.003

Iwashina T, Uehara A, Kitajima J, Yukawa T (2015) Anthocyanins and other flavonoids from Amorphophallus titanum having largest inflorescence in plant kingdom, and other two species. Bull Natl Museum Nat Sci Ser B 41:33–44

Izar GM, Morais LG, Pereira CDS et al (2019) Quantitative analysis of pellets on beaches of the São Paulo coast and associated non-ingested ecotoxicological effects on marine organisms. Reg Stud Mar Sci 29:100705. https://doi.org/10.1016/j.rsma.2019.100705

Johansen DA (1940) Plant microtechnique. McGraw-Hill Book Company Inc, London, p 530p

Klumpp A, Klumpp G, Domingos M (1994) Plants as bioindicators of air pollution at the serra do mar near the industrial complex of Cubatão, Brazil. Environ Pollut 85:109–116. https://doi.org/10.1016/0269-7491(94)90244-5

Lallemand LA, Zubieta C, Lee SG et al (2012) A structural basis for the biosynthesis of the major chlorogenic acids found in coffee. Plant Physiol 160:249–260. https://doi.org/10.1104/pp.112.202051

Leiss KA, Maltese F, Choi YH et al (2009) Identification of chlorogenic acid as a resistance factor for thrips in chrysanthemum. Plant Physiol 150:1567–1575. https://doi.org/10.1104/pp.109.138131

Long ER, Macdonald DD, Smith SL, Calder FD (1995) Incidence of adverse biological effects within ranges of chemical concentrations in marine and estuarine sediments. Environ Manage 19:81–97. https://doi.org/10.1007/BF02472006

Lüttge U (2010) Ability of crassulacean acid metabolism plants to overcome interacting stresses in tropical environments. AoB Plants. https://doi.org/10.1093/aobpla/plq005

Mao B, Zhao L, Zhao Q, Zeng D (2018) Effects of ultraviolet (UV) radiation and litter layer thickness on litter decomposition of two tree species in a semi-arid site of Northeast China. J Arid Land 10:416–428. https://doi.org/10.1007/s40333-018-0054-6

Masyita A, Mustika Sari R, Dwi Astuti A et al (2022) Terpenes and terpenoids as main bioactive compounds of essential oils, their roles in human health and potential application as natural food preservatives. Food Chem X 13:100217. https://doi.org/10.1016/j.fochx.2022.100217

Moreira FT, Balthazar-Silva D, Barbosa L, Turra A (2016) Revealing accumulation zones of plastic pellets in sandy beaches. Environ Pollut 218:313–321. https://doi.org/10.1016/j.envpol.2016.07.006

Moreira LB, Leite PRBD, de Dias ML et al (2019) Sediment quality assessment as potential tool for the management of tropical estuarine protected areas in SW Atlantic, Brazil. Ecol Indic 101:238–248. https://doi.org/10.1016/j.ecolind.2018.12.052

Morris JK (1965) A formaldehyde glutaraldehyde fixative of high osmolality for use in electron microscopy. J Cell Biol 27:1A-149A

Neves NR, Oliva MA, da Cruz CD et al (2009) Photosynthesis and oxidative stress in the restinga plant species Eugenia uniflora L. exposed to simulated acid rain and iron ore dust deposition: potential use in environmental risk assessment. Sci Total Environ 407:3740–3745. https://doi.org/10.1016/j.scitotenv.2009.02.035

O'Brien TP, Feder N, McCully ME (1964) Polychromatic staining of plant cell walls by toluidine blue O. Protoplasma 59:368–373. https://doi.org/10.1007/BF01248568

Olsen JT, Caudle KL, Johnson LC et al (2013) Environmental and genetic variation in leaf anatomy among populations of Andropogon gerardii (Poaceae) along a precipitation gradient. Am J Bot 100:1957–1968. https://doi.org/10.3732/ajb.1200628

Parmar TK, Rawtani D, Agrawal YK (2016) Bioindicators: the natural indicator of environmental pollution. Front Life Sci 9:110–118. https://doi.org/10.1080/21553769.2016.1162753

Petracco M, Camargo RM, Berenguel TA et al (2015) Evaluation of the use of Olivella minuta (Gastropoda, Olividae) and Hastula cinerea (Gastropoda, Terebridae) as TBT sentinels for sandy coastal habitats. Environ Monit Assess 187:440. https://doi.org/10.1007/s10661-015-4650-z

Piccinelli AL, Campone L, Dal Piaz F et al (2009) Fragmentation pathways of polycyclic polyisoprenylated benzophenones and degradation profile of nemorosone by multiple-stage tandem mass spectrometry. J Am Soc Mass Spectrom 20:1688–1698. https://doi.org/10.1016/j.jasms.2009.05.004

Pinheiro MAA, Duarte LFA, Toledo TR et al (2013) Habitat monitoring and genotoxicity in Ucides cordatus (Crustacea: Ucididae), as tools to manage a mangrove reserve in southeastern Brazil. Environ Monit Assess 185:8273–8285. https://doi.org/10.1007/s10661-013-3172-9

Rahman S, Mehta S, Husen A (2023) Plants and their unexpected response to environmental pollution: an overview. In: Husen ABTP (ed) Plants and their interaction to environmental pollution. Elsevier, Amsterdam, pp 1–23

Rocha C, Bergallo H, Van Sluys M et al (2007) The remnants of restinga habitats in the brazilian Atlantic Forest of Rio de Janeiro state, Brazil: habitat loss and risk of disappearance. Brazilian J Biol 67:263–273. https://doi.org/10.1590/S1519-69842007000200011

Rocha-Filho LC, Krug C, Silva CI, Garófalo CA (2012) Floral resources used by euglossini bees (Hymenoptera: Apidae) in coastal ecosystems of the Atlantic Forest. Psyche A J Entomol 2012:1–13. https://doi.org/10.1155/2012/934951

Scarano FR (2009) Plant communities at the periphery of the Atlantic rain forest: rare-species bias and its risks for conservation. Biol Conserv 142:1201–1208. https://doi.org/10.1016/j.biocon.2009.02.027

Siqueira-Silva AI, da Silva LC, Azevedo AA, Oliva MA (2012) Iron plaque formation and morphoanatomy of roots from species of restinga subjected to excess iron. Ecotoxicol Environ Saf 78:265–275. https://doi.org/10.1016/j.ecoenv.2011.11.030

Skorupinska-Tudek K, Poznanski J, Wojcik J et al (2008) Contribution of the mevalonate and methylerythritol phosphate pathways to the biosynthesis of dolichols in plants. J Biol Chem 283:21024–21035. https://doi.org/10.1074/jbc.M706069200

Soares AMS, Oliveira JTA, Rocha CQ et al (2018) Myracrodruon urundeuva seed exudates proteome and anthelmintic activity against Haemonchus contortus. PLoS ONE 13:e0200848. https://doi.org/10.1371/journal.pone.0200848

Tangerina MMP, Cesário JP, Pereira GRR et al (2018) Chemical profile of the sulphated saponins from the starfish luidia senegalensis collected as by-Catch Fauna in Brazilian Coast. Nat Products Bioprospect 8:83–89. https://doi.org/10.1007/s13659-018-0153-2

Taniguchi S, Colabuono FI, Dias PS et al (2016) Spatial variability in persistent organic pollutants and polycyclic aromatic hydrocarbons found in beach-stranded pellets along the coast of the state of São Paulo, southeastern Brazil. Mar Pollut Bull 106:87–94. https://doi.org/10.1016/j.marpolbul.2016.03.024

Tomašević M, Vukmirović Z, Rajšić S et al (2008) Contribution to biomonitoring of some trace metals by deciduous tree leaves in urban areas. Environ Monit Assess 137:393–401. https://doi.org/10.1007/s10661-007-9775-2

Vieira-Filho MS, Lehmann C, Fornaro A (2015) Influence of local sources and topography on air quality and rainwater composition in Cubatão and São Paulo, Brazil. Atmos Environ 101:200–208. https://doi.org/10.1016/j.atmosenv.2014.11.025

Yang L, Wen K-S, Ruan X et al (2018) Response of plant secondary metabolites to environmental factors. Molecules 23:762. https://doi.org/10.3390/molecules23040762

Zhang Y, Shi P, Qu H, Cheng Y (2007) Characterization of phenolic compounds inErigeron breviscapus by liquid chromatography coupled to electrospray ionization mass spectrometry. Rapid Commun Mass Spectrom 21:2971–2984. https://doi.org/10.1002/rcm.3166